

## Impacts of urban morphology on sensible heat flux and net radiation exchange



Jinxin Yang <sup>a</sup>, Zhifeng Wu <sup>a,\*</sup>, Massimo Menenti <sup>b,c</sup>, Man Sing Wong <sup>d</sup>, Yanhua Xie <sup>e</sup>, Rui Zhu <sup>f</sup>, Sawaiid Abbas <sup>d,g,h</sup>, Yong Xu <sup>a</sup>

<sup>a</sup> School of Geography and Remote Sensing, Guangzhou University, Guangzhou 510006, China

<sup>b</sup> Faculty of Civil Engineering and Earth Sciences, Delft University of Technology, P. O. Box 5048, Delft 2600, GA, Netherlands

<sup>c</sup> State Key Laboratory of Remote Sensing Science, Institute of Remote Sensing and Digital Earth, Chinese Academy of Sciences, Beijing 100101, China

<sup>d</sup> Land Surveying and Geo-Informatics, Faculty of Construction and Environment, The Hong Kong Polytechnic University, Hung Hom, Kowloon, Hong Kong, SAR, China

<sup>e</sup> Nelson Institute Center for Sustainability and the Global Environment (SAGE), University of Wisconsin-Madison, 1710 University Avenue, Madison, WI 53726, USA

<sup>f</sup> Institute of High Performance Computing (IHPC), Agency for Science, Technology and Research (A\*STAR), 1 Fusionopolis Way, Singapore, 138632, Republic of Singapore

<sup>g</sup> Smart Sensing for Climate and Development, Centre for Geographical Information System, University of the Punjab, Lahore, Pakistan

<sup>h</sup> Remote Sensing, GIS and Climatic Research Lab (RSGCRL), National Center of GIS and Space Applications, University of the Punjab, Lahore, Pakistan

### ARTICLE INFO

#### Keywords:

Urban geometry  
Urban heat exchange  
Urban heat mitigation  
Urban sensible heat flux  
Building density  
Net radiation

### ABSTRACT

Urban morphology affects the sensible heat flux and net radiation exchange which can alter urban heat mitigation plans. This study first parameterized the geometric effects on the net radiation, and then calculated the net radiation and sensible heat flux in the urban landscape of Hong Kong. Considering that the sensible heat flux is the main heat sink in compact urban areas, this study proposes a Normalized Urban Sensible Heat Mitigation Index (NUSHMI) based on the ratio of the net radiation and sensible heat flux. Overall, there is major difference in the dependence of net radiation and sensible heat flux on geometric parameters. Net radiation  $R_n$  reaches an optimal value, either maximum or minimum depending on the parameters of SVF and a standard deviation of building height  $\sigma_h$ , at intermediate parameter values, which suggests a guideline relevant to urban design targeting the mitigation of urban climate. Contrariwise, sensible heat flux decreases or increases, again depending on SVF and  $\sigma_h$ , being considered, with increasing values of the same parameters. For example,  $R_n$  reaches a minimum value for a Sky View Factor (SVF) between 0.5 and 0.6, while it reaches a maximum value for a standard deviation of building height  $\sigma_h$  between 20 and 30 m. These two results suggest that radiative forcing, i.e.  $R_n$ , can be minimized by urban space with SVF around 0.55 and  $\sigma_h$  around 25 m. The relationships between sensible heat flux and SVF or  $\sigma_h$  do not show multiple minima or maxima (as with  $R_n$ ), with the exception of building density, which could also be applied as a guideline in urban design. The results based on the proposed NUSHMI indicated the NUSHMI reaches the highest values when building density is about 0.7 and building height is about 80 m and when the building height

\* Corresponding author.

E-mail addresses: [yangjx11@gzhu.edu.cn](mailto:yangjx11@gzhu.edu.cn) (J. Yang), [zfwu@gzhu.edu.cn](mailto:zfwu@gzhu.edu.cn) (Z. Wu), [m.menenti@tudelft.nl](mailto:m.menenti@tudelft.nl) (M. Menenti), [lswong@polyu.edu.hk](mailto:lswong@polyu.edu.hk) (M.S. Wong), [xie78@wisc.edu](mailto:xie78@wisc.edu) (Y. Xie), [zhur@ihpc.a-star.edu.sg](mailto:zhur@ihpc.a-star.edu.sg) (R. Zhu), [sawaiid.gis@pu.edu.pk](mailto:sawaiid.gis@pu.edu.pk), [sawaiid.rsgcrl@pu.edu.pk](mailto:sawaiid.rsgcrl@pu.edu.pk) (S. Abbas), [xu1129@gzhu.edu.cn](mailto:xu1129@gzhu.edu.cn) (Y. Xu).

standard deviation within an area is about 10 m to 20 m. These findings revealed how the urban morphology affects the surface heat flux exchange between urban canopy and atmosphere boundary layer, and can help to design an efficient urban landscape towards urban heat mitigation for highly compacted cities, e.g. controlling the building density, height, and the height deviation. This combination of urban geometric parameters identifies an urban configuration maximizing the dissipation of absorbed radiant energy as sensible heat. It should be noted, however, that heat load upon buildings would be reduced at the price of maximizing heat dissipation within the built-up space.

## 1. Introduction

The urban surface energy balance determines the urban surface and air temperature (Oke, 1982). The radiative energy absorbed by the urban surface must be dissipated as latent heat flux, if water is available, sensible heat flux by warming the surface layer and by heat storage in urban objects. The dissipation of the radiative energy in excess of latent heat, forces the surface and air temperature to adjust heat fluxes at the urban surface balance each other, as dictated by the 1st principle of thermodynamics, i.e. the surface energy balance. These processes determine the magnitude of the radiative and convective energy exchanges within the built-up environment, i.e. the urban climate. To achieve thermodynamic equilibrium, these fluxes determine the values of state variables, such as air and surface temperature, taking into account system properties such as thermal properties and aerodynamic roughness. Understanding the interactions between the urban canopy and the atmosphere is central to monitoring and understanding urban climate and environment and also provides guidelines for urban design (Ward et al., 2014). Urban land cover combined with geometry makes the urban surface energy exchange different from rural areas. Radiation trapping by built-up areas increases the absorption of shortwave radiation and reduces long-wave radiation loss (Arnfield, 1990; Harman et al., 2004; Kastendeuch and Najjar, 2009; Yang and Li, 2015). Urban geometry has a large impact on turbulent heat dissipation because buildings act as blocks to alter wind speed in all directions in the urban canopy, which increases the spatial variability in sensible heat flux at building facets (Hang et al., 2009; Yang and Li, 2015). These processes may change the local microclimate of urban areas and then increase the urban surface temperature.

Generally, higher vegetation cover can mitigate urban heat (Kuang et al., 2015; Weng et al., 2004) because of transpiration and evaporation. Urban geometry can also have positive impacts on the thermal environment in an urban area e.g. by shading streets and pedestrians (Lindberg and Grimmond, 2011; Yu et al., 2019). Additionally, the nonuniform building pattern increases the aerodynamic roughness of the urban canopy, which may increase the sensible heat dissipation to some degree. These processes may reduce the surface temperature. Thus, it is vital to systematically understand the comprehensive effects of urban geometry on urban heat exchange in urban landscapes.

The urban surface energy balance can be written as:  $Q^*(\text{net radiation}) + Qf(\text{anthropogenic heat}) = Qh(\text{sensible heat}) + Qe(\text{latent heat}) + Qg(\text{ground heat})$ . Several studies showed that the sensible heat flux is the main heat sink in compact urban areas (Fig. 6.17 in Oke et al., 2017; Christen and Vogt, 2004; Grimmond et al., 2004). In some urban areas with high vegetation abundance, the latent heat can be similar in magnitude to sensible heat (Abunnasr et al., 2022; Grimmond and Oke, 1999b), while the latent heat flux over compact built-up areas is relatively low because of the low vegetation abundance. Sensible heat is directly related to urban heat mitigation (Yang et al., 2016) and urban energy consumption (Yu et al., 2020). Net radiation flux is the key driver of surface energy exchange (Ao et al., 2016). The net radiation is not only affected by background climate conditions, but also affected by local geometry because of the blocking and shading. Other radiative and convective heat fluxes are also affected by the 3D urban geometry, i.e. shortwave and longwave irradiance, reflected radiance, latent and ground heat fluxes. Reflected radiance and ground heat are also affected by urban materials (Chrysoulakis et al., 2018; Offerle et al., 2006). Ao et al. (2016) analyzed trends in radiative fluxes using measurements gathered in Shanghai and results showed that solar elevation and azimuth angle had a large effect on the shortwave radiation because of shadow casting. In summary, net radiation is the energy absorbed by the built-up space, thus it is the forcing driving the processes that determine urban climate. The absolute and relative magnitudes of the remaining radiative and convective fluxes are determined by urban geometry, materials and land cover, and by the prevailing conditions including wind speed, boundary layer stability and vapour pressure deficit. Sensible heat remains the main mode of dissipating excess energy, i.e. the difference between net radiation and latent heat plus anthropogenic heat, given atmospheric boundary conditions.

Sensible heat flux is the most important sink of urban surface energy, with urban geometry having complex effects on both urban net radiation (source) and sensible heat flux (sink) (Yu et al., 2020). With regard to net radiation, the urban geometry affects both shortwave and longwave irradiance onto urban canyon facets. Multiple reflection and scattering reduce exitance at the top of the urban canopy by trapping reflected shortwave radiance and longwave emittance (Yang and Li, 2015). Additionally, the shadows caused by urban geometry make the estimation of absorbed solar irradiance more complex (Lindberg et al., 2015; Tian et al., 2019). The total area of building facets receiving solar irradiance is much larger than a horizontal, flat surface because of the 3D structure of the built-up space. These combined processes determine the net radiation in the urban canopy.

With regards to sensible heat flux, the geometry changes the aerodynamic roughness of the urban surface and changes the resistance to sensible heat flux transfer from urban canopy to atmosphere (Grimmond, 1998). The average daytime Bowen ratio (ratio of the sensible heat flux to the latent heat flux) can reach 4.4 in a sparsely vegetated area to 9.8 in an urban center (Grimmond and Oke, 2002). Generally, vegetation is useful for urban heat mitigation (Wang et al., 2022), but in dense and compact cities, e.g., Hong Kong, vegetation cover is rather scarce (Yang et al., 2022). Thus, the sensible heat flux is the main heat sink (Wong et al., 2015). Less net

radiation and more sensible heat dissipation means less surface heat storage within the urban canopy, which improves cooling of the built-up space (Yang et al., 2016). Then the sensible heat flux is heating the urban boundary layer, thus dispersing a large fraction of absorbed radiative energy and reducing the heat absorbed by the urban surface and by the urban surface layer. The design of urban space can minimize net radiation and maximize sensible heat flux, thus mitigating the urban excess heat and reduce urban temperature.

Understanding how the urban geometry affects the urban surface energy exchange is essential for urban heat mitigation, which requires information about the optimal spatial configuration of urban buildings to enhance heat dissipation and reduction of heat storage (Ando and Ueyama, 2017). How the urban geometry affects the urban surface temperature was studied by a number of numerical experiments (Chen et al., 2020; Krayenhoff and Voogt, 2007; Yang and Li, 2015), and also the effects of geometry on sensible heat flux and radiation balance were addressed by previous studies (Coutts et al., 2007; Crawford et al., 2018; Krayenhoff and Voogt, 2007; Martilli, 2014). (Vallati et al., 2017) showed that the urban canopy street configuration may increase 22.1% to 67.6% heating or cooling demand because of the radiative interreflections in shortwave and longwave fields between the facades of a building. Those studies indicated that the urban geometric characteristics have complex effects on urban surface energy exchange. However, more in-depth investigation on how urban geometries may mitigate or intensify urban heat excess has not been performed yet.

Here we relate mitigation of the heat load upon the built-up space to the dissipation of excess radiant energy by maximizing sensible heat exchange. We regard excess energy as being the difference between net radiation and latent heat flux plus anthropogenic heat. In Hong Kong, our study area, urban vegetation is rather scarce, thus latent heat exchange is rather small. Anthropogenic heat is likewise a rather small fraction of net radiation. Accordingly, in this first study we regard net radiation only as the excess energy to be dissipated in urban areas. Further, we regard the minimization of heat load upon buildings as most relevant to reduce energy consumption and improve comfort in the inner built-up space. Dissipation by sensible heat transfer, however, increases heat transferred to the urban boundary layer, i.e. higher air temperature. Our overall goal was to understand how heat dissipation relates to the configuration of urban space, i.e. to urban geometric properties. Any such relationship should be replicable in and applicable to different urban areas and different environmental conditions. Accordingly, we developed and evaluated a normalized index based on the ratio of sensible heat flux to net radiation. A normalized index was adopted because the surface heat fluxes are affected heavily by the urban configuration and by background climate conditions. Thus, the absolute magnitude of sensible heat and net radiation fluxes vary very significantly across urban areas and do not lead to easily applicable results. Accordingly, our specific objective was to evaluate a normalized index as a generally applicable metric of energy dissipation by sensible heat in urban areas. We have

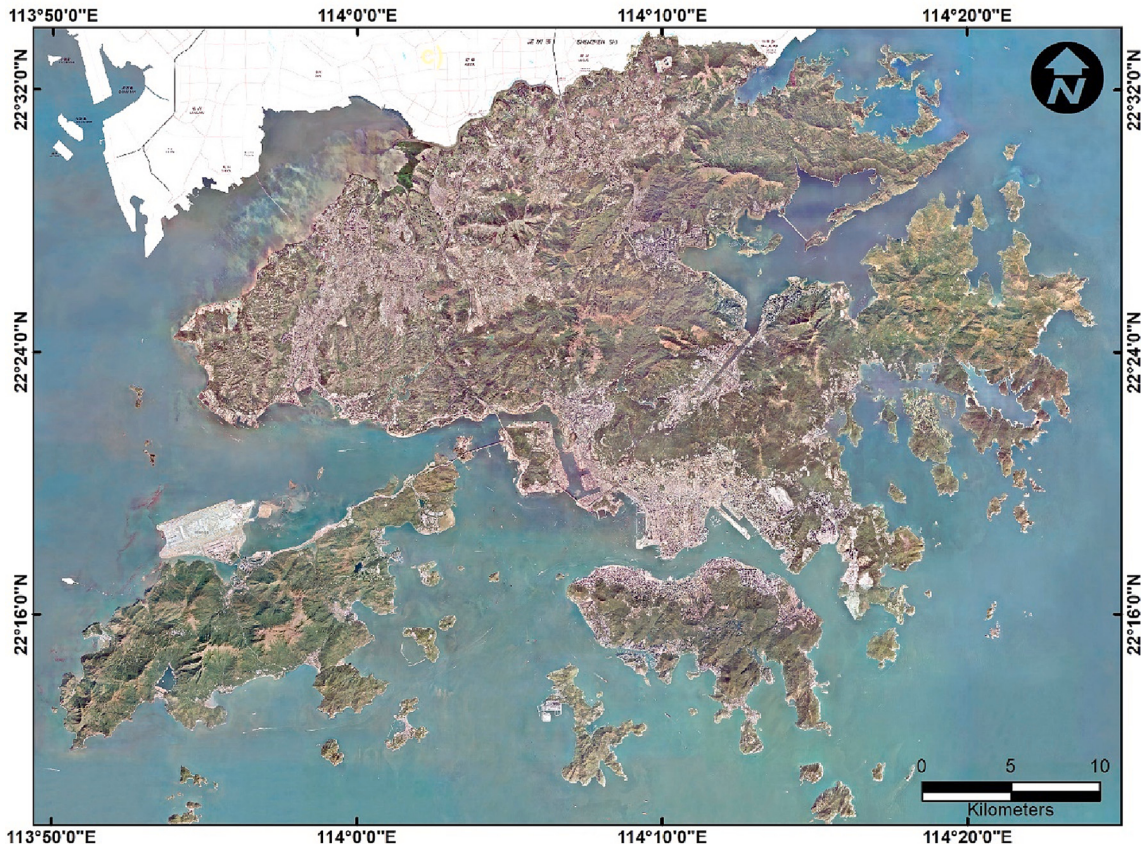


Fig. 1. Map of study area.

investigated the relationships between sensible heat flux and net radiation in response to the building geometric parameters, e.g., building density, building height and building height variation, to characterize the heat mitigation efficiency under different geometric conditions. For this purpose, the net radiation and sensible heat flux from 2010 to 2011 over urban areas in Hong Kong were estimated using Landsat data and geometry data first, then the proposed normalized heat mitigation index was calculated and interpreted in several different climate cases and geometry conditions. This study will help reveal what kind of urban geometric characteristics are helpful for heat mitigation in compact urban areas like Hong Kong.

## 2. Study area and data

### 2.1. Study area

This study was focused on the urban areas of Hong Kong (Fig. 1). Urban building density and height were retrieved from a 1 m spatial resolution Digital Surface Model (Fig. 2c and d). The net radiation and sensible heat flux were calculated for the entire area shown in Fig. 1, while the detailed analysis on the relation between heat fluxes and urban geometry was only carried out for the areas with building density larger than 0. Hong Kong is a high-density city located on the coastline of Southeast China ( $22^{\circ}17'N$ ,  $114^{\circ}09'E$ ). The elevation of the city ranges from sea level to 957 m with an average altitude of 8 m (Chen et al., 2012). Buildings in the urban areas are in a compact setting (Fig. 2 c), which results in Hong Kong reaching one of the highest net built-up densities in the world.

### 2.2. Data background and preprocessing

The geometric parameters used in this study include building density, building height, building height standard deviation (difference) within 30 m grid and Sky View Factor (SVF) which were derived from an airborne Light Detection and Ranging (LiDAR) based high resolution (1 m) Digital Surface Model (DSM) and building GIS data, obtained from the Hong Kong Civil Engineering and Development Department and Hong Kong Lands Department (Lai et al., 2012) (Fig. 2). The LiDAR data was collected during December 2010 and January 2011 and the vertical data accuracy is about 3 cm root mean square (rms) on clear flat ground. The DSM (Fig. 2a) and building GIS data were used to calculate and map the SVF (Fig. 2b), building density (Fig. 2c) and the building height standard

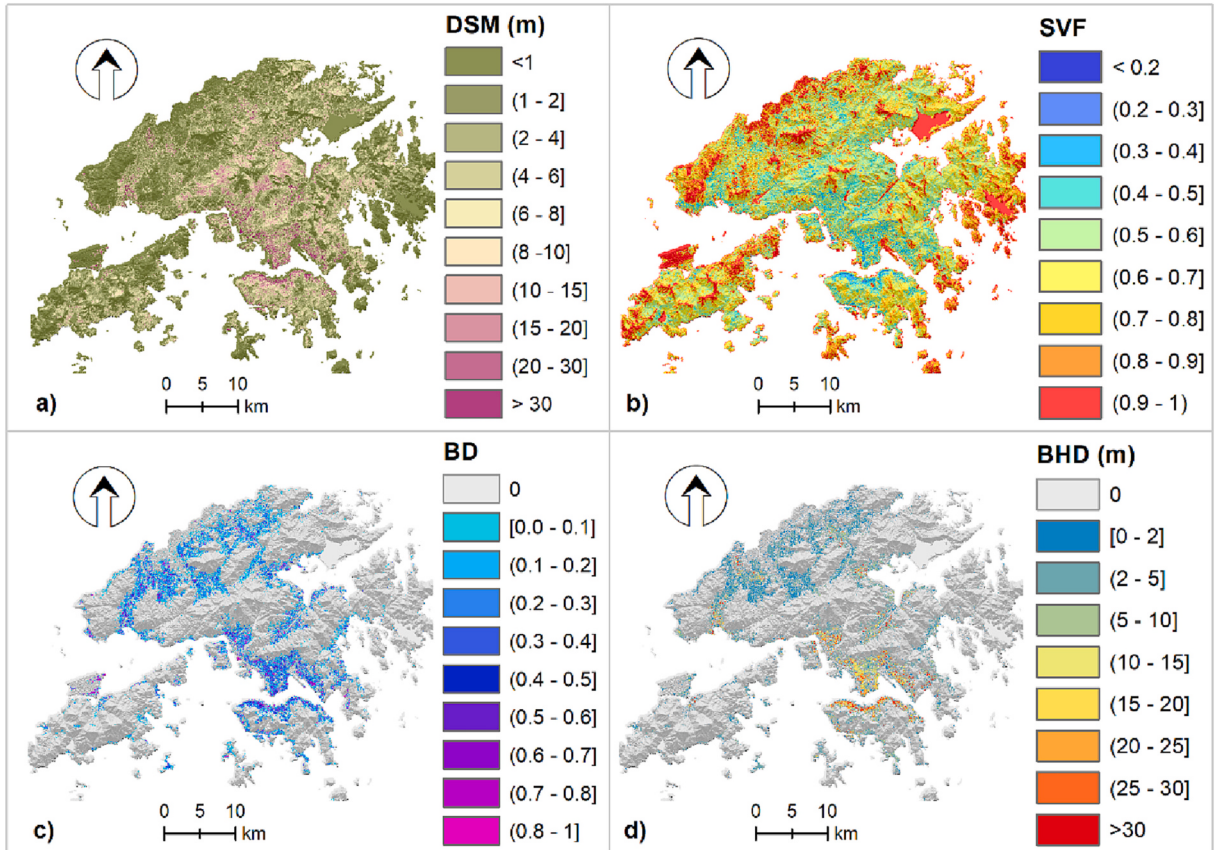


**Fig. 2.** Urban morphology data used in this study; a) Digital Surface Model (DSM), b) Sky view Factor (SVF), c) building density (BD), and d) building height standard deviation (BHD).

deviation (Fig. 2d) of Hong Kong. The land cover classification data from the Hong Kong Planning Department and building GIS data were used to obtain the material emissivity in the study area. The classification data include the impervious surface, grass, shrubland and woodland. The building GIS shapefile data were used to separate the buildings and flat areas from the impervious surface. The land use and land cover classification data were acquired from the Hong Kong Planning Department and the overall classification accuracy in urban areas was 96% according to the Hong Kong Planning Department (Yang et al., 2015b). The material emissivity calculation is based on the urban material emissivity library provided by (Kotthaus et al., 2014) and more information about the DSM, building data, land cover classification data and emissivity estimation can be found in Yang et al. (2015a).

Concurrent Landsat satellite data with LiDAR data were collected to estimate the net radiation and sensible heat flux. The surface reflectance and the surface temperature products of Landsat C2L2 were used to retrieve the surface temperature based on Yang et al. (2015b) in this study. Four cloudless images observed on Oct 29 2010, Dec 23 2010, Mar 13 2011 and Jun 1 2011 were obtained from the Earth Explorer (<https://earthexplorer.usgs.gov/>). To analyze the effects of geometry on the net radiation and sensible heat fluxes, the net radiation and sensible heat fluxes were first estimated based on Landsat data, urban building height/density, and atmospheric data. The spatial resolution of the Landsat data used in this study was 30 m (after downscaling the thermal band data), thus the net radiation and sensible heat flux estimates apply to 30 m pixels. Both fluxes are defined at the interface between the urban surface and the atmosphere, so a calculation at the relatively high spatial resolution is meaningful and reflects the heterogeneity of the land surface. This high spatial resolution approach is widely documented in literatures (Abunnasr et al., 2022; Xu et al., 2008; Yu et al., 2020). From the perspective of direct measurements by e.g. a tower-mounted eddy-covariance device, the source area of the measured turbulent fluxes is much larger and variable with weather conditions and might even be asymmetric because of wind direction and speed. It is a well-established practice to evaluate remote sensing estimates of turbulent heat fluxes using tower-based measurements (Kuang et al., 2015; Park et al., 2012). The issue is then the delineation of the dynamic footprint of the measurements towards spatial integration of the estimates, many studies document the moderate to good agreement of Landsat based estimates of sensible heat flux with tower-based measurement (Feigenwinter et al., 2018). Accordingly, the 30 m grid was deemed adequate to estimate and map sensible heat flux.

### 3. Method

To analyze the effects of geometry on the net radiation and sensible heat fluxes, the net radiation and sensible heat fluxes were first estimated based on Landsat data, urban building height/density, and atmospheric data.

The net radiation is mainly affected by shadow and radiative transfer within urban canopy. The shadow fraction determines the received direct solar radiation and the sky view factor (SVF) determines the received diffuse solar and atmospheric radiation. Additionally, the SVF also affects the upwelling longwave radiation from urban canopy. Thus, the relationship between the pixelwise net radiation and urban geometry can be expressed as:

$$R_n = (1 - \alpha)^*(F_s K_{dir} + SVF^* \lambda_c^* K_{dif}) + SVF^* \lambda_c^* \epsilon_e^* \epsilon_a \sigma^* T_a^4 - \epsilon_e^* \sigma^* T_s^4 \quad (1)$$

where  $\alpha$  is the albedo, calculated from the surface reflectance according to the Landsat products and the method of Liang (2001),  $F_s$  is the sunlit fraction of horizontal surface,  $K_{dir}$  is the direct solar radiation and measured by Hong Kong Observatory,  $F_s K_{dir}$  is the direct solar radiation received by the surface. For direct sunlight, only the sunlit part of a horizontal surface needs to be considered. Direct sunlight on vertical walls is negligible, given the shadows and the high sun elevation in HK. SVF is the average Sky View Factor (SVF) of bottom, rooftops and wall in the 30 m scale. The SVF was first calculated for both bottom and rooftop facets at the spatial resolution of the DSM, i.e. 1 m. The SVF used for further analyses is the mean Sky View Factor (SVF) of bottom and rooftop facets within each 30 m grid scale. The SVF at 1 m spatial resolution was calculated from DSM data based on the method by (Kokalj et al., 2011) and the calculation evaluated the blocking by adjacent buildings in 32 directions within a radius of 100 m. The SVF of wall facets was calculated using the method of Yang et al. (2015a). Then the SVF at 1 m spatial resolution of all facets within each 30 m grid were averaged.  $\lambda_c$  is the ratio of the complete facet area of a building to the horizontal planar area, calculated with the GIS building data (Yang et al., 2020), the diffuse solar irradiance is assumed isotropic and homogeneous at the top of the urban canopy over the entire study area, as measured at the Hong Kong Observatory. Diffuse radiance can reach the facets of urban buildings and it has been calculated as described by Eq. 1. The amount of received diffuse solar radiation is determined by the SVF estimated as ( $SVF^* \lambda_c^* K_{dif}$ );  $\epsilon_e$  is the effective emissivity, calculated based on the land cover data, building data and SVF according to Yang et al. (2015a),  $\epsilon_e$  included the multiple scattering within the pixels of wall and other facets, thus the longwave contribution from wall scattering within the pixels has been included.  $\epsilon_a$  is the atmosphere emissivity, and calculated by the relative humidity and atmosphere temperature based on Kato and Yamaguchi (2005).  $T_a$  is the air temperature at 100 m above ground level, simulated by numerical simulation model WRF and the spatial resolution is 1 km.  $T_s$  is the urban surface radiometric temperature retrieved from Landsat TM data based on the method developed by (Yang et al., 2015b) and included the multiple scattering and adjacent pixel effects,  $SVF^* \lambda_c^* \epsilon_e^* \epsilon_a \sigma^* T_a^4$  is the received longwave radiation from atmosphere, and  $\epsilon_e^* \sigma^* T_s^4$  is the upwelling longwave radiation. The calculation applies to the volume defined horizontally by the 30 m grid and vertically by the top of the urban canopy, including the wall, roof and bottom facets within each grid.

The sensible heat flux was calculated as

$$H = \rho C_p \frac{T_s - T_a}{r_{ah} + r_r} \quad (2)$$

where  $r_{ah}$  is the aerodynamic resistance for heat transfer and can be written as (Verma, 1989):

$$r_{ah} = \frac{1}{ku_*} \left[ \ln\left(\frac{z - z_d}{z_{0m}}\right) + \ln\left(\frac{z_{0m}}{z_{0h}}\right) - \psi_H \right] \quad (3)$$

where  $k$  is the Von Karman's constant (0.4),  $u_*$  is the friction velocity (m/s), and  $\psi_H$  is the stability correction for heat.  $z$  is the height of the wind speed and air temperature measurements (m);  $z_d$  is the zero-plane displacement height (m),  $z_{0m}$  is the roughness length for momentum (m),  $z_{0h}$  is the roughness length for heat (m). The friction velocity,  $u_*$  is given by the stability corrected log-law as:

$$u_* = U k \left[ \ln\left(\frac{z - z_d}{z_{0m}}\right) + \psi_m \left( \frac{z - z_d}{L} \right) - \psi_m \left( \frac{z_{0m}}{L} \right) \right]^{-1} \quad (4)$$

where  $U$  is the wind speed,  $\psi_m$  is the stability correction for momentum.

$r_r$  is the radiometric excess resistance (s/m) and calculated as:

$$r_r = B^{-1} u_*^{-1} \quad (5)$$

and  $B^{-1} = k^{-1} \ln\left(\frac{z_{0m}}{z_{0h}}\right)$ ,

$$\text{and } z_{0h} = z_{0m} [7.4 \exp(-1.29 Re_*^{0.25})] \quad (6)$$

where  $Re_* = z_{0m} u_* / v$  can be as  $1.461 \times 10^{-5}$  m/s (Xu et al., 2008).

$z_{0m}$  and  $z_d$  were calculated using Raupach (1994) method as described by (Grimmond and Oke, 1999a). Eq. 6 is also widely used to estimate the sensible heat flux in urban areas (Voogt and Grimmond, 2000; Xu et al., 2008). This parameterization method has been used in previous studies of sensible heat flux estimation in Hong Kong with reasonable results (Wong et al., 2015; Yang et al., 2019; Yang et al., 2016).

Eqs. 1 to 6 suggest that the geometric characteristics have complex effects on sensible and net radiation. This explains why it remains a challenge to describe explicitly the effects of geometry on urban heat mitigation. To understand these effects on urban heat mitigation, a normalized urban sensible heat mitigation index (NUSHMI) was proposed in this study:

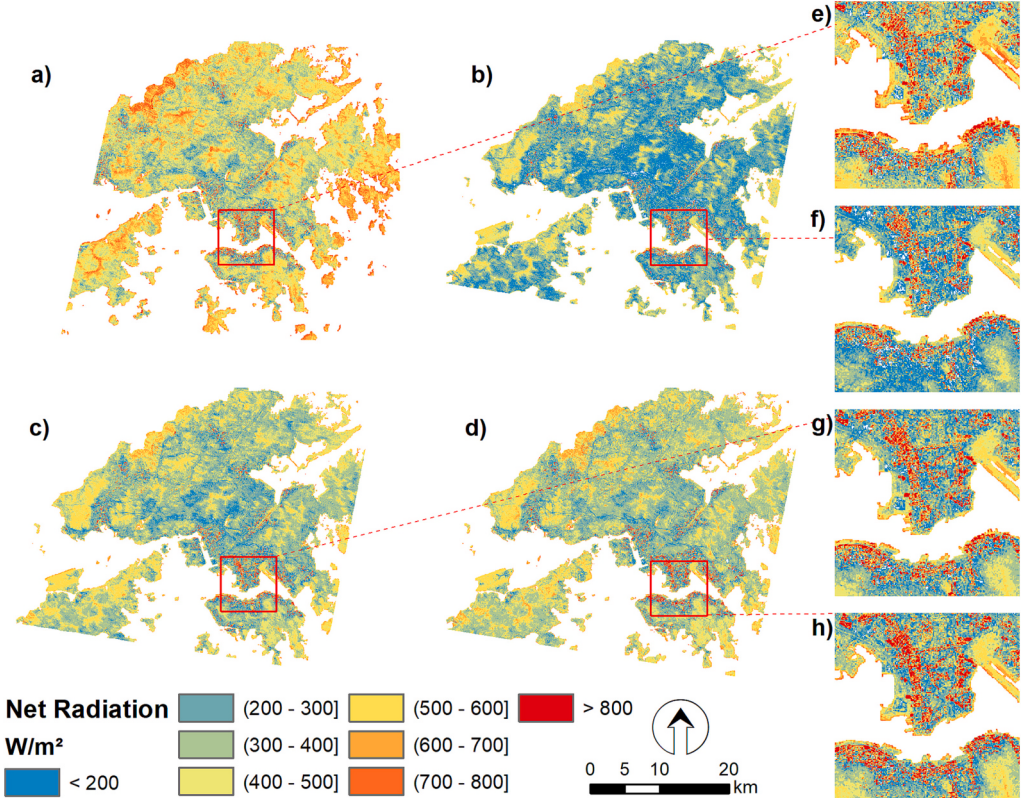
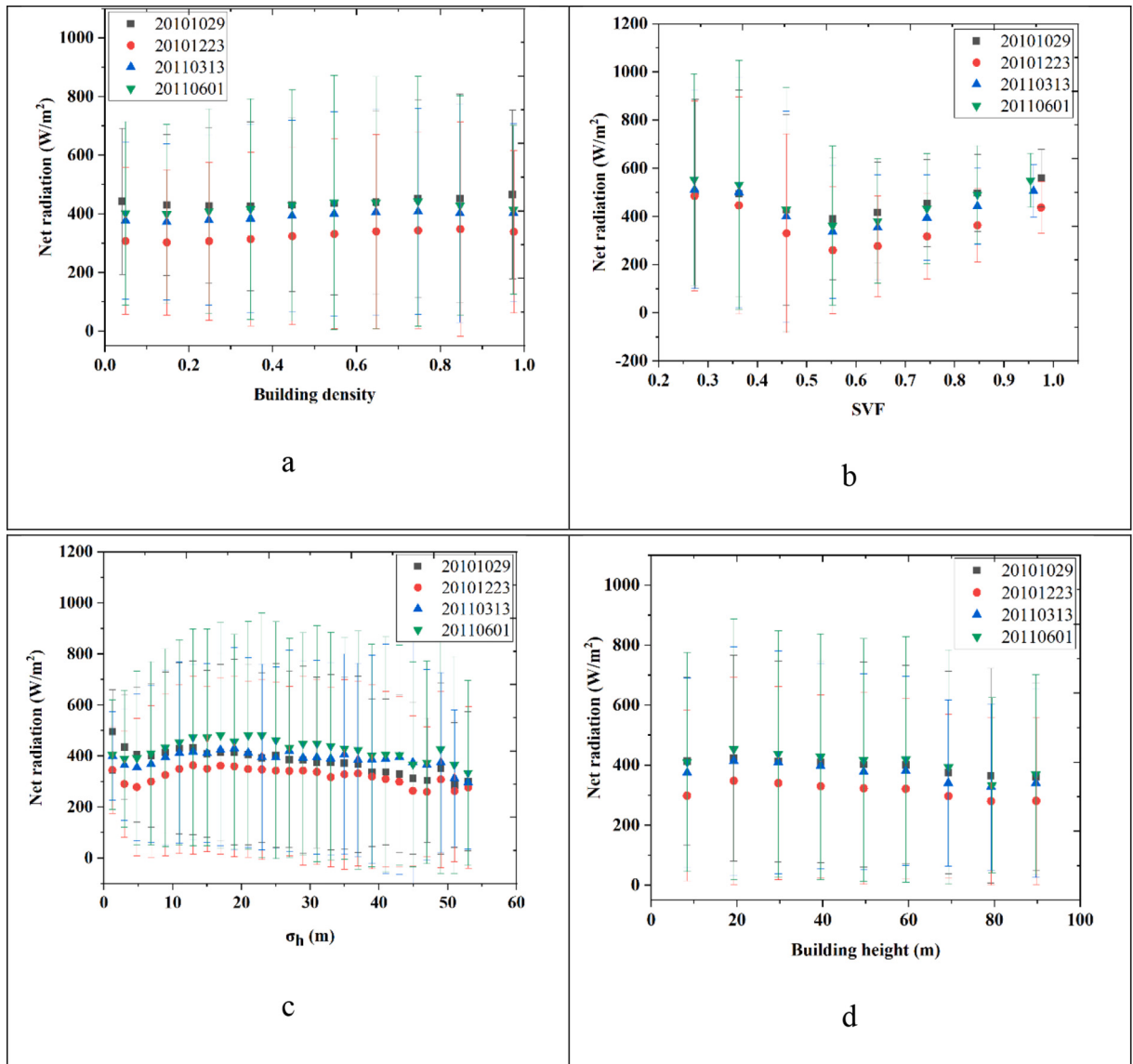


Fig. 3. Net radiation acquired on different dates: a) Oct 29, 2010; b) Dec 23, 2010; c) Mar 13, 2011; d) Jun 1, 2011.

$$NUSHMI = \frac{\frac{H}{Rn} - (\frac{H}{Rn})_{min}}{(\frac{H}{Rn})_{max} - (\frac{H}{Rn})_{min}} \quad (7)$$

$(\frac{H}{Rn})_{max}$  and  $(\frac{H}{Rn})_{min}$  is taken from the entire domain, i.e. the  $(\frac{H}{Rn})_{min}$  is from rural areas, which makes the H/Rn values in urban area easier to understand when compared with same  $(\frac{H}{Rn})_{min}$ .  $(\frac{H}{Rn})_{max} - (\frac{H}{Rn})_{min}$  is the range of the ratio of the sensible heat flux to net radiation condition and means the range of sensible heat mitigation rate under certain background. The NUSHMI is a metric of the efficiency of an urban patch to dissipate excess energy, taken equal to net radiation in this study. Indicates the sensible heat mitigation rate at such background, and ranges from 0 to 1. When NUSHMI is close to 0, the sensible heat mitigation is minimum. When the NUSHMI is close to 1, the sensible heat mitigation is maximum. The metric is generic as defined, since it normalizes differences in H and Rn by applying their ratio and it normalizes the variability of the ratio by applying a minimum and a maximum values = of the ratio of heat flux densities. In order to study the geometry effects on the heat fluxes and the heat mitigation, linear relationships between paired building geometric parameters (including building density, building height, SVF and building height variation) and heat fluxes were studied.



**Fig. 4.** Relationship between net radiation and geometric parameters: a) building density (BD), b) Sky view Factor (SVF), c) building height deviation (BHD) and d) building height. (Values plotted are averages of all image samples (see Fig. 3) within a bin equal to 0.1 (a), 0.1 (b), 3 m (c) and 10 m (d)).

## 4. Results

### 4.1. Effects of geometry on net radiation

The net radiation ( $R_n$ ) in different seasons (Fig. 3) was calculated using Eq. 1. The results showed that the net radiation in built-up areas is higher than that in flat areas. Although building shadows reduce the direct solar irradiance, wall facets in compact built-up areas absorb diffuse radiation. In Hong Kong, buildings are compact and narrow. This results in a built-up area, including walls, much larger than the flat area, i.e., the effects of walls in urban energy exchange cannot be neglected. The results in Fig. 3 show that diffuse radiation absorbed by wall facets cannot be neglected in urban areas. These results matched well with the simulated net radiation from TUF3D model in Table 5.4 from Oke, 1982, the net radiation of built-up areas can increase about 28% compared with flat facets of comparable materials.

The effects of geometry on net radiation are illustrated by Fig. 4. Results show that the net radiation increases with building density when building density is between 0.2 and 0.8 in winter, spring and summer (Fig. 4a). When building density is smaller than 0.2 and larger than 0.8, the net radiation decreases with increasing building density. When building density is too small, increasing some buildings adds shadows, while the absorbed diffuse radiation by wall facets is less than the reduction in direct solar radiation caused by shadows. Thus, the net radiation decreases with increasing building density when the building density is small (< 0.2). While the direct solar radiation on wall facets is not considered, and this may slightly affect the results. When building density is larger than 0.2, the area of wall facets increases significantly. The increase in absorbed radiation by wall facets is larger than the reduction in direct solar radiation caused by shadows. When building density is larger than 0.8, compact buildings reduce the incoming diffuse solar and longwave radiation. The results indicated that the diffuse radiation by wall facets also has significant effects on urban heat exchange. The solar radiation is affected by the combination of solar azimuth/elevation with urban geometry. On October 29, 2010 in autumn, the trend of net radiation with building density is similar with other seasons, decreasing with building density first and then increased with building density (Fig. 4a). Only the threshold value for building density was slightly different in the winter, spring and summer. The net radiation decreased with SVF when SVF was smaller than 0.6 and reached the minimum when SVF was about 0.5 to 0.6. Then, the net radiation increased with the increase of SVF when SVF was larger than 0.6 (Fig. 4b). When SVF is small, the buildings are compact and the area of wall facets accounts for a significant part of the absorption of diffuse solar radiation. When SVF is smaller than

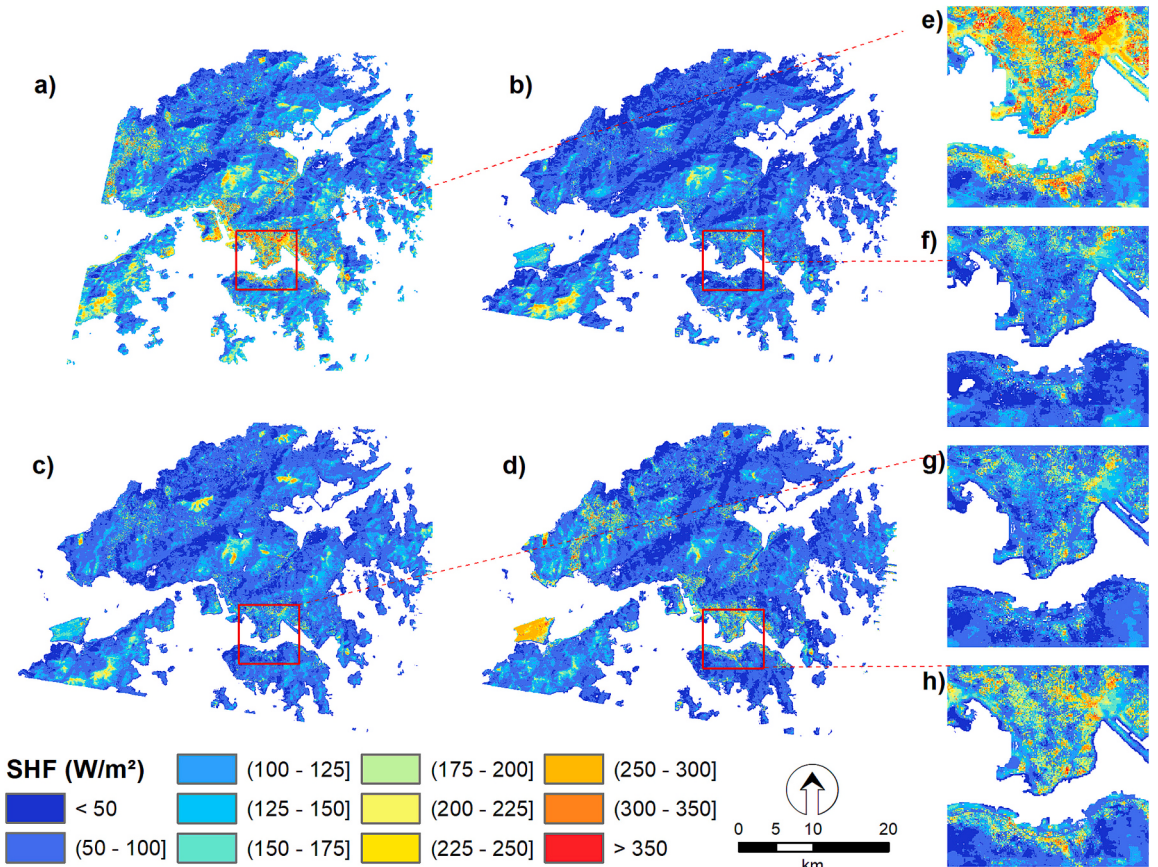
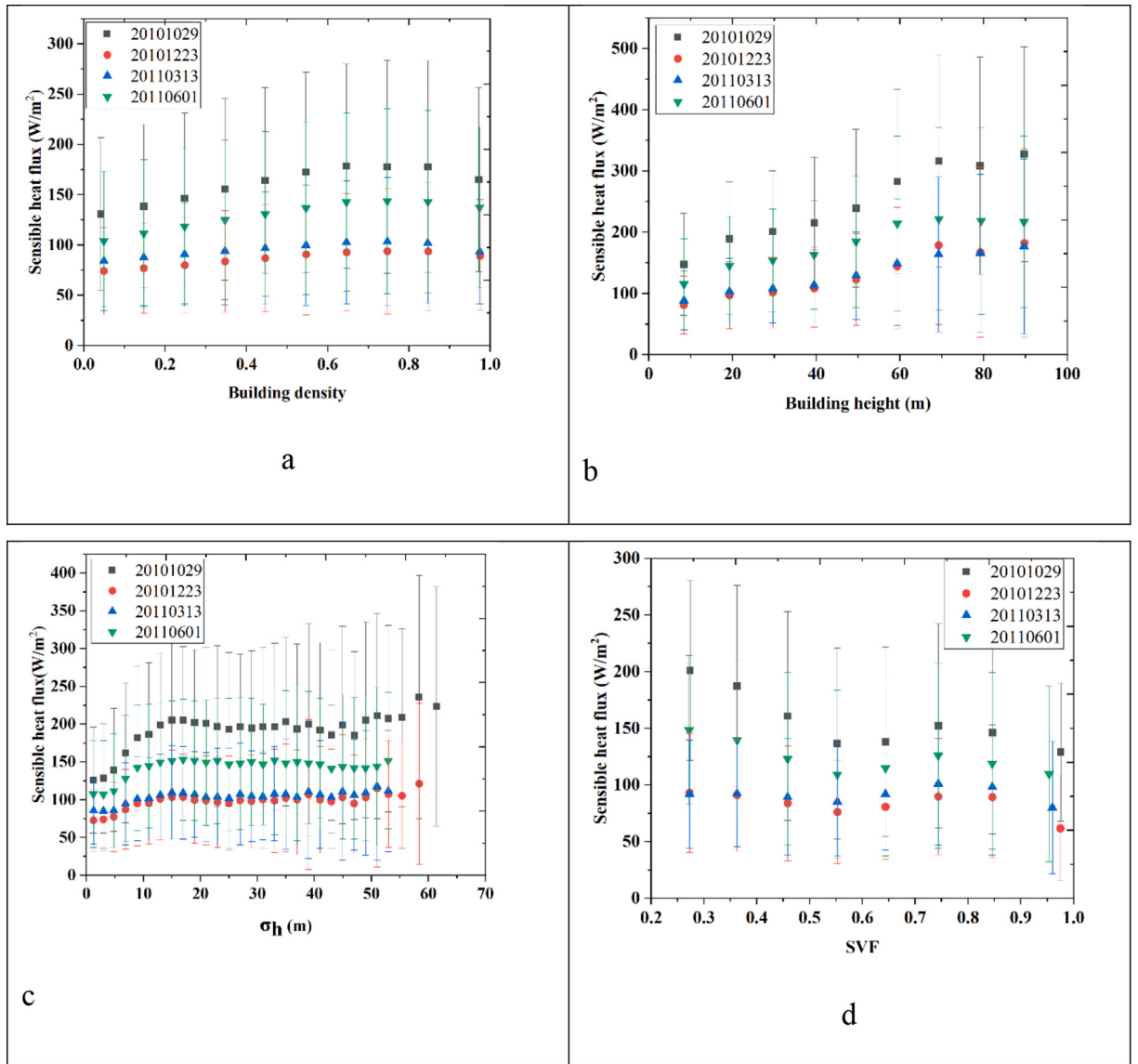


Fig. 5. Sensible heat flux in different seasons: a) Oct 292,010; b) Dec 232,010; c) Mar 132,011; d) Jun 12,011.

0.5, the building density is still the dominant factor for net radiation because of the diffuse radiation absorbed by wall facets. When SVF is higher than 0.6, the net radiation is determined by the horizontal facets.

The net radiation increases with the spatial variability of building height when the standard deviation of building height,  $\sigma_h$ , in an area is smaller than about 15 m (Fig. 4c). This is because a larger variability in building height increases the exposure of wall facets to diffuse radiation. When  $\sigma_h$  is between 15 m and 40 m, the net radiation decreases slightly with an increasing  $\sigma_h$ , while the net radiation decreases when  $\sigma_h > 40$  m. This is because shadows become dominant factors of net radiation due to the larger variability in building height. The relationship between net radiation and building height is similar to the relationship with  $\sigma_h$ . When building height is smaller than 20 m, the net radiation increases with building height (Fig. 4d). This is because the increased wall facet area due to higher buildings is the dominant factor in these conditions. When the building height is between 20 m and 50 m, the effects of geometry on net radiation are similar. When the building height is higher than 50 m, the wall facet area increased, leading to a decrease of SVF simultaneously. This results in a decrease of net radiation with the building height when building height is higher than 50 m. The observed relationships between geometric parameters and net radiation indicate that the complex effects of geometry on net radiation cannot be neglected.



**Fig. 6.** Relationship between sensible heat flux and geometric parameters: a) building density (BD), b) Sky view Factor (SVF), c) building height deviation (BHD) and d) building height. (Values plotted are averages of all image samples (see Fig. 3) within a bin equal to 0.1 (a), 0.1 (b), 3 m (c) and 10 m (d)).

#### 4.2. Effects of geometry on sensible heat flux

The sensible heat flux in urban areas is higher in autumn and summer than in winter and spring (Fig. 5). In October and June buildings in Hong Kong still need cooling. In December and March neither cooling or heating is necessary because of the warm winter in Hong Kong. This increases the urban surface temperature and then contributes to a higher sensible heat flux in October and June than in December and March. Particularly,  $R_n$  was much higher in October and June (Fig. 3) than in December and March, i.e. the amount of absorbed energy to be dissipated was much higher in October and March, thus explaining the higher sensible heat flux. The effects of geometric parameters on sensible heat flux are also very complex. We studied the relationships between sensible heat fluxes and individual geometric parameters to understand the effect of geometry on sensible heat flux (Fig. 6). Results showed that the sensible heat flux increases with building density  $b_x$  when  $b_x < 0.7$  (Fig. 6a). When building density is higher than 0.7, the sensible heat flux decreases with increasing building density. When building density increases, the displacement height increases, which can reduce the aerodynamic resistance. Therefore, the sensible heat flux increases with  $b_x$  when  $b_x < 0.7$ . When  $b_x > 0.7$ , airflow passing through

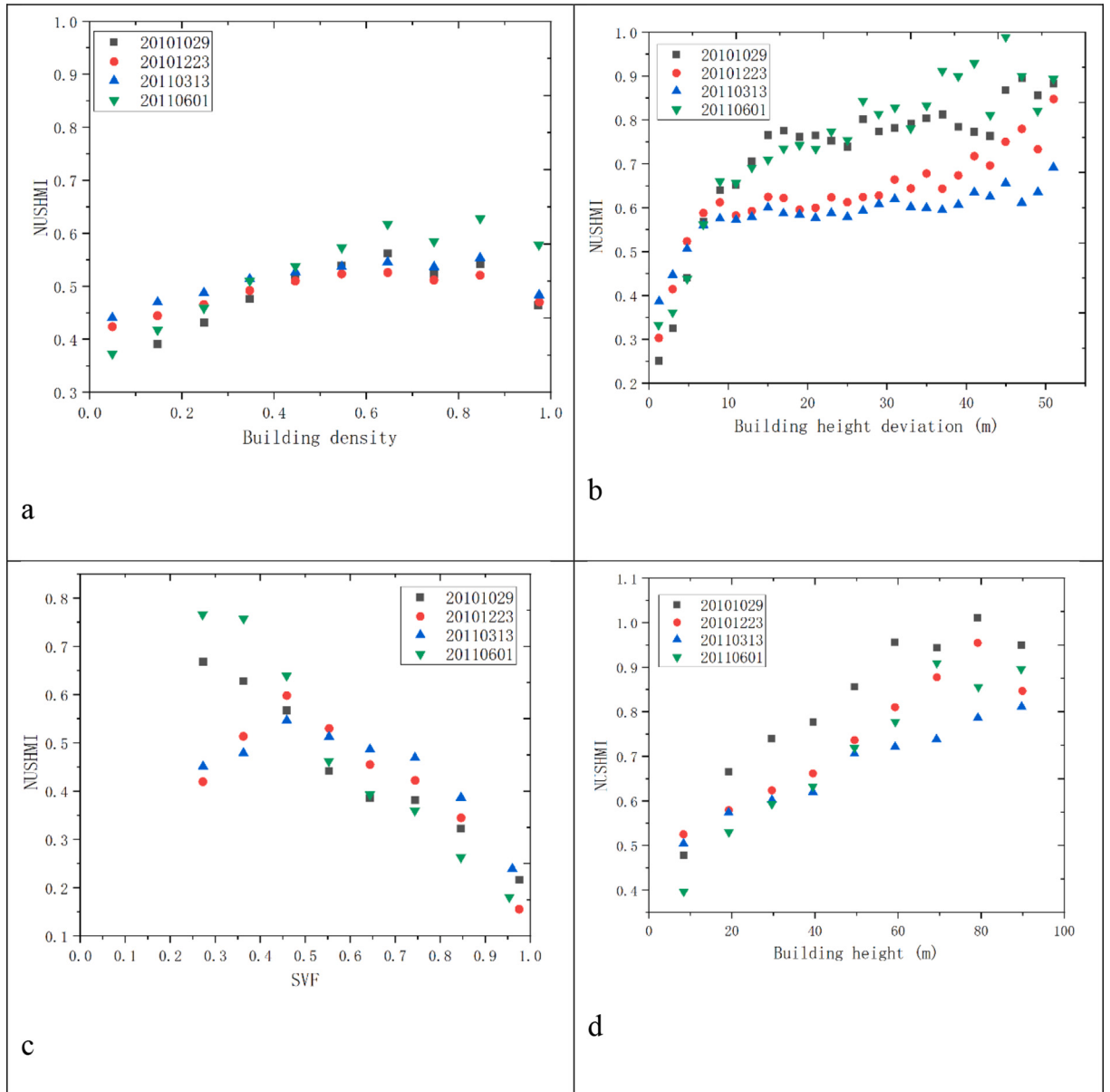


**Fig. 7.** Relationship between NUSHMI and geometric parameters: a) building density (BD), b) Sky view Factor (SVF), c) building height deviation (BHD) and d) building height. (Values plotted are averages of all image samples (see Fig. 3) within a bin equal to 0.1 (a), 0.1 (b), 3 m (c) and 10 m (d)).

the built-up area is reduced, making sensible heat flux decrease with  $b_x$ . Consequently,  $b_x = 0.7$  appears to be a threshold because it is a turning point on maximizing sensible heat flux. Note that sensible heat flux also increases with building height  $h_b$  when it is shorter than 70 m, most likely due to the increase in the displacement height. The latter leads to a lower aerodynamic resistance, thus a higher sensible heat flux. Results also showed that the threshold value of the building height is 70 m (Fig. 6b). When  $h_b > 70$  m, the sensible heat flux tends to a constant. When  $\sigma_h$  changes, the sensible heat flux increases first when  $\sigma_h < 15$  m, while when  $\sigma_h > 15$  m, there is no clear relationship between sensible heat flux and  $\sigma_h$ . The threshold value  $\sigma_h$  appears to be 15 m (Fig. 6c). When SVF increases, the sensible heat flux firstly decreases when  $SVF < 0.6$ . With  $0.5 < SVF < 0.6$ , the sensible heat flux reaches a minimum value, then it increases with SVF when  $0.6 < SVF < 0.8$ . When  $SVF > 0.8$ , the sensible heat flux decreases with SVF (Fig. 6d).

#### 4.3. Effects of geometry on $H/R_n$

This study investigated the relationship between NUSHMI (Eq. 7) and geometric parameters (Fig. 7). The results showed that the effects of  $b_x$  on NUSHMI are similar in different seasons when  $b_x < 0.7$  (Fig. 7a). NUSHMI increases with  $b_x$  when  $b_x < 0.7$ , while when  $b_x \approx 0.7$ , the NUSHMI reaches a maximum value, after which NUSHMI decreases with increasing  $b_x$ . This indicates that heat mitigation by increasing sensible heat flux can reach maximum when  $b_x \approx 0.7$ . The effects of  $\sigma_h$  on NUSHMI are similar in different seasons when  $\sigma_h < 10$  m (Fig. 7b). The NUSHMI increases with  $\sigma_h$  in winter and spring when  $\sigma_h < 10$  m. In autumn and summer, the inflection point in the  $\sigma_h$  versus NUSHMI relationship is  $\sigma_h \approx 20$  m. Then, the NUSHMI has no obvious change until  $\sigma_h \approx 40$  m, while NUSHMI increases slightly when  $\sigma_h > 40$  m.

In autumn and summer, NUSHMI decreases with increasing SVF (Fig. 7c). In the winter and spring, NUSHMI increases with the increase of SVF when  $SVF < 0.5$ , while NUSHMI decreases with an increasing SVF when  $SVF > 0.5$  in a similar way in different seasons. The NUSHMI increases with  $h_b$  when  $h_b < 70$  m (Fig. 7d).

## 5. Discussion

The urban geometry affects the urban surface energy exchange and then affects the urban thermal environment. Thus, numerous studies analyzed the effects of geometry on urban surface energy exchange from different perspectives based on numerical models (Harman et al., 2004; Kanda et al., 2007; Krayenhoff and Voogt, 2007). These studies mostly analyzed geometry effects on one or two energy exchange parameters, e.g. albedo or solar irradiance.

This study proposed a new parameterization of the wall effects on net radiation in urban areas, although the estimation of the effects of wall shadows on direct solar radiation have not yet been incorporated. The wall areas for diffuse radiation must be considered in compact built-up areas like Hong Kong urban areas, thus we separated the direct and diffuse solar radiation and estimated the diffuse solar radiation absorbed by walls. The latter was parameterized using a wall area index and SVF, which appeared to be effective indices to estimate diffuse solar irradiance and atmospheric emittance absorbed by wall facets. The results also showed that the wall facets have significant effects on net radiation. In the built-up areas, the net radiation is higher than in flat wide areas, although the flat wide-open areas have less shadow and can receive more direct solar radiation, but the wall facets of built-up areas absorb a large amount of diffuse radiation. This means that the wall effects cannot be neglected when estimating urban net radiation and studying the urban surface energy exchange. (Chatzipoulka et al., 2016) analyzed the urban geometry on the solar radiation availability and results showed that the solar radiation availability within urban canopy varied with building density, building height and building height deviation. In this study, the net radiation is affected by building density, building height and building deviation and SVF. The building density, building height and building height deviation affects the availability of the direct solar radiation. The SVF affects the diffuse solar and longwave irradiance onto urban facets. Sharmin et al. (2017) showed using the ENVI-met numerical model that the variable building height reduces the solar gain within the urban canopy. In this study, the net radiation decreased with the building height difference first, and then tended to a constant value. This means the results in this study are comparable with other studies.

To estimate the sensible heat flux, this study adopted the methods proposed by Voogt and Grimmond (2000) and Grimmond and Oke (1999a), and considered the geometry effects based on DSM, building data and land cover classification data. The surface temperature was retrieved by applying the method developed by Yang et al. (2015b) taking the urban geometry into account to estimate the effective emissivity of the built-up space. The retrieved surface temperature was used directly to estimate the sensible heat flux. We did not apply the cold/hot pixel method, as in Bastiaanssen et al. (1998), to estimate the surface to air temperature difference. The foundation of this method is that the lower reference temperature (cold pixel) is determined by latent heat flux, which is negligible in the urban areas of Hong Kong. Moreover, in the small and fragmented vegetation patches, the surface to air temperature difference is strongly affected by heat advection, while the cold/warm pixel concept relies on the assumption that this difference is determined by the local heat fluxes. Compared with previous studies mostly based on land cover data, our estimates of sensible heat flux can capture and represent the geometry effects in urban areas. Thus, we also studied the relationship between each geometric parameter and sensible heat flux. Results showed that the sensible heat flux can reach the maximum value when the building density is about 0.7 and the standard deviation of building height is about 15 m. In the study of Kanda and Moriizumi (2009), the effects of building height variation on sensible heat flux were analyzed and the buildings were simple scaled uniform models ( $0.15\text{ m} \times 0.15\text{ m} \times 0.075\text{ m}$  and  $0.15\text{ m} \times 0.15\text{ m} \times 0.225\text{ m}$ ) and the height of the blocks were set as 0.075 m and 0.225 m. In this condition, the sensible heat flux was insensitive to building height variation. In this study, when the building height variation is higher than 15 m to 20 m, the sensible heat flux appears to be insensitive to urban height variation. In the study of, the sensible heat flux was insensitive to a doubling in building height. From this sense, the results in this study are comparable.

To reveal the complex effects of geometry on sensible heat and net radiation fluxes, the best conditions for urban heat mitigation

needs to take into account the relationships between sink heat fluxes and source heat fluxes. Considering that sensible heat flux is the main sink of absorbed radiative energy in compact urban areas, this study proposed a normalized index, i.e., NUSHMI, the ratio of sensible heat flux to the net radiation. The relationship between the NUSHMI and geometric parameters revealed how the urban geometry contributes to heat mitigation by dissipation of sensible heat flux. There are several urban heat mitigation indices proposed in literature, e.g., the temperature difference caused by vegetation change (Krayenhoff et al., 2021). These heat mitigation indices did not consider the relationship between urban geometry and urban surface energy exchange. The sensible heat mitigation index proposed in this study considers the relation between urban geometry and urban surface energy exchange, and the results document that the NUSHMI is sensitive to urban geometry. The relationship between geometric parameters and the NUSHMI showed that the effects of building density on the NUSHMI is insensitive to the seasonal condition or background climate conditions. The effects of building height variation on NUSHMI is also insensitive to different seasonal conditions when building height variation is smaller than 10 m. When SVF is larger than 0.5, NUSHMI is also insensitive to seasonal change. The relationship between geometric parameters and the NUSHMI showed that the effects of building density on the NUSHMI is insensitive to the seasonal condition or background climate conditions. The effects of building height variation on NUSHMI is also insensitive to different seasonal conditions when building height variation is smaller than 10 m. When SVF is larger than 0.5, NUSHMI is also insensitive to seasonal change. This is shown by comparing Figs. 4 (Rn) and 6 (H) with Fig. 7 (NUSHMI), where the values of the fluxes and of NUSHMI are plotted versus the urban geometry parameters considered in this study. It appears that the large seasonal variability in heat fluxes is almost completely removed by applying NUSHMI. The latter suggests that NUSHMI is indeed an effective metric of the impact of urban morphology. There is a notable exception, namely the difference between NUHSMI values in the relationship with the building height deviation during the colder and warmer seasons (Fig. 7 b). This finding requires further study. This means the NUSHMI can be used to normalize the variability of net radiation and sensible heat flux caused by different climate conditions and evaluate the urban heat mitigation under different seasonal or climate conditions. Increasing the urban heat mitigation can reduce the energy consumption of urban space and help the urban areas to cool down naturally. This study can be used to help develop guidelines for urban planning for urban heat mitigation.

There are several limitations in this study. The estimated net radiation and sensible heat flux were not validated. This is because there is no ground measurement data available on heat fluxes in Hong Kong. At the same time, the geometric data were not available in other areas to replicate our analysis. We have studied the surface heat fluxes over Hong Kong earlier (Wong et al., 2015; Yang et al., 2019; Yang et al., 2016). Results from these previous studies showed that the method applied to estimate sensible heat flux in this study is appropriate to estimate sensible heat flux in Hong Kong urban areas (Yang et al., 2016). This study mainly analyzed the variations in the net radiation and sensible heat flux caused by different geometry to determine approximate design guidelines towards urban heat mitigation.

This study is based on data acquired in different seasons, thus we explored a range of variability in the radiative forcing of urban climate. On the other hand, all our observations were in daytime, while nighttime urban climate is forced by radiative cooling and the effect of buildings might be significantly different. We will explore such differences in a new study.

## 6. Conclusion

Quantifying the effects of urban geometry on urban heat flux exchange provides an opportunity to better understand how to mitigate urban heat load. This study first parameterized the geometry effects on net radiation, and then calculated net radiation and sensible heat flux in Hong Kong urban areas. The relationships between geometric parameters and sensible heat flux and net radiation were studied, and results showed that when SVF is about 0.5 to 0.6, the net radiation and sensible heat flux reach the minimum values. When building density is about 0.7, the net radiation and sensible heat flux reach their maximums. Considering that the sensible heat flux in compact urban areas is the main sink of absorbed radiative energy, this study proposed a normalized heat mitigation index based on the ratio of sensible heat flux to net radiation (NUSHMI). The relationships between geometry and NUSHMI showed that when building density is about 0.7 and building height is about 80 m, the NUSHMI obtains the maximum value. When the standard deviation of the building height is about 10 m to 20 m, the NUSHMI attains the maximum values. The discovered phenomenon and patterns can support urban design towards creating a comfortable urban thermal environment.

## CRediT authorship contribution statement

**Jinxin Yang:** Conceptualization, Data curation, Funding acquisition, Investigation, Methodology, Project administration, Resources, Software, Supervision, Validation, Visualization, Writing – original draft, Writing – review & editing. **Zhifeng Wu:** Conceptualization. **Massimo Menenti:** Conceptualization, Writing – review & editing. **Man Sing Wong:** Data curation, Funding acquisition. **Yanhua Xie:** Writing – review & editing. **Rui Zhu:** Writing – review & editing. **Sawaiid Abbas:** Visualization. **Yong Xu:** Writing – review & editing.

## Declaration of Competing Interest

The authors declare no conflict of interest.

## Data availability

The authors do not have permission to share data.

## Acknowledgement

This work was supported by Grants by National Natural Science Foundation of China (42271345), Guangdong Provincial Natural Science Foundation (2021A1515012567). The authors thank the Hong Kong Planning Department, Hong Kong Lands Department, the Hong Kong Civil Engineering and Development Department, the Hong Kong Observatory and the Hong Kong Government Flying Service for the planning, building GIS, weather and climate, and airborne Lidar data. Massimo Menenti acknowledges the support by the Chinese Academy of Sciences President's International Fellowship Initiative (grant no. 2020VTA0001), the MOST High Level Foreign Expert program (Grant nr. GL20200161002) and grant P10-TIC-6114 by the Junta de Andalucía. M.S. Wong thanks the funding support from the General Research Fund (Grant No. 15603920 and 15609421), and the Collaborative Research Fund (Grant No. C5062-21GF) from the Research Grants Council, Hong Kong, China.

## References

- Abunnasr, Y., Mhawej, M., Chrysoulakis, N., 2022. SEBU: a novel fully automated Google earth engine surface energy balance model for urban areas. *Urban Clim.* 44, 101187.
- Ando, T., Ueyama, M., 2017. Surface energy exchange in a dense urban built-up area based on two-year eddy covariance measurements in Sakai, Japan. *Urban Clim.* 19, 155–169.
- Ao, X., et al., 2016. Radiation fluxes in a business district of Shanghai, China. *J. Appl. Meteorol. Climatol.* 55 (11), 2451–2468.
- Arnfield, A.J., 1990. Canyon geometry, the URBAN fabric and nocturnal cooling: a simulation approach. *Phys. Geogr.* 11 (3), 220–239.
- Bastiaanssen, W., Menenti, M., Feddes, R., Holtslag, A., 1998. A remote sensing surface energy balance algorithm for land (SEBAL). 1. Formulation. *J. Hydrol.* 212, 198–212.
- Chatzipoula, C., Compagnon, R., Nikolopoulou, M., 2016. Urban geometry and solar availability on façades and ground of real urban forms: using London as a case study. *Sol. Energy* 138, 53–66.
- Chen, L., Ng, E., An, X., Ren, C., Lee, M., Wang, U., He, Z., 2012. Sky view factor analysis of street canyons and its implications for daytime intra-urban air temperature differentials in high-rise, high-density urban areas of Hong Kong: a GIS-based simulation approach. *Int. J. Climatol.* 32, 121–136.
- Chen, Y., Wu, J., Yu, K., Wang, D., 2020. Evaluating the impact of the building density and height on the block surface temperature. *Build. Environ.* 168, 106493.
- Christen, A., Vogt, R., 2004. Energy and radiation balance of a central European city. *Int. J. Climatol.* 24 (11), 1395–1421.
- Chrysoulakis, N., et al., 2018. Urban energy exchanges monitoring from space. *Sci. Rep.* 8 (1), 11498.
- Coutts, A.M., Beringer, J., Tapper, N.J., 2007. Impact of increasing urban density on local climate: spatial and temporal variations in the surface energy balance in Melbourne, Australia. *J. Appl. Meteorol. Climatol.* 46 (4), 477–493.
- Crawford, B., et al., 2018. Variability of urban surface temperatures and implications for aerodynamic energy exchange in unstable conditions. *Q. J. R. Meteorol. Soc.* 144 (715), 1719–1741.
- Feigenwinter, C., et al., 2018. Spatial distribution of sensible and latent heat flux in the City of Basel (Switzerland). *IEEE J. Select. Top. Appl. Earth Observat. Remote Sens.* 11 (8), 2717–2723.
- Grimmond, C., 1998. Aerodynamic roughness of urban areas derived from wind observations. *Bound.-Layer Meteorol.* 89 (1), 1–24.
- Grimmond, C., Oke, T.R., 1999a. Aerodynamic properties of urban areas derived from analysis of surface form. *J. Appl. Meteorol.* 38 (9), 1262–1292.
- Grimmond, C., Oke, T.R., 1999b. Heat storage in urban areas: local-scale observations and evaluation of a simple model. *J. Appl. Meteorol.* 38 (7), 922–940.
- Grimmond, C., Oke, T.R., 2002. Turbulent heat fluxes in urban areas: observations and a local-scale urban meteorological parameterization scheme (LUMPS). *J. Appl. Meteorol.* 41 (7), 792–810.
- Grimmond, C., Salmon, J., Oke, T.R., Offerle, B., Lemonsu, A., 2004. Flux and turbulence measurements at a densely built-up site in Marseille: heat, mass (water and carbon dioxide), and momentum. *J. Geophys. Res.-Atmos.* 109 (D24).
- Hang, J., Sandberg, M., Li, Y., 2009. Effect of urban morphology on wind condition in idealized city models. *Atmos. Environ.* 43 (4), 869–878.
- Harman, I., Best, M., Belcher, S., 2004. Radiative exchange in an urban street canyon. *Bound.-Layer Meteorol.* 110 (2), 301–316.
- Kanda, M., Kanega, M., Kawai, T., Moriwaki, R., Sugawara, H., 2007. Roughness lengths for momentum and heat derived from outdoor urban scale models. *J. Appl. Meteorol. Climatol.* 46 (7), 1067–1079.
- Kanda, M., Morizumi, T., 2009. Momentum and Heat Transfer over Urban-like Surfaces. *Boundary-Layer Meteorology* 131, 385–401.
- Kastendeuch, P.P., Najjar, G., 2009. Simulation and validation of radiative transfers in urbanised areas. *Sol. Energy* 83 (3), 333–341.
- Kato, S., Yamaguchi, Y., 2005. Analysis of urban heat-island effect using ASTER and ETM+ Data: Separation of anthropogenic heat discharge and natural heat radiation from sensible heat flux. *Remote Sensing of Environment* 99, 44–54.
- Kokalj, Ž., Zaksek, K., Oštrir, K., 2011. Application of sky-view factor for the visualisation of historic landscape features in lidar-derived relief models. *Antiquity* 85 (327).
- Kotthaus, S., Smith, T.E.L., Wooster, M.J., Grimmond, C.S.B., 2014. Derivation of an urban materials spectral library through emittance and reflectance spectroscopy. *ISPRS J. Photogramm. Remote Sens.* 94 (0), 194–212.
- Krayenhoff, E.S., Voogt, J., 2007. A microscale three-dimensional urban energy balance model for studying surface temperatures. *Bound.-Layer Meteorol.* 123 (3), 433–461.
- Krayenhoff, E.S., et al., 2021. Cooling hot cities: a systematic and critical review of the numerical modelling literature. *Environ. Res. Lett.* 16 (5), 053007.
- Kuang, W., et al., 2015. Quantifying the heat flux regulation of metropolitan land use/land cover components by coupling remote sensing modeling with in situ measurement. *J. Geophys. Res.-Atmos.* 120 (1), 113–130.
- Lai, A., So, A.C., Ng, S., Jonas, D., 2012. The Territory-Wide Airborne Light Detection and Ranging Survey for the Hong Kong Special Administrative Region. In The 33RD Asian Conference on Remote Sensing 26–30.
- Liang, S., 2001. Narrowband to broadband conversions of land surface albedo I: algorithms. *Remote Sens. Environ.* 76 (2), 213–238.
- Lindberg, F., Grimmond, C.S.B., 2011. The influence of vegetation and building morphology on shadow patterns and mean radiant temperatures in urban areas: model development and evaluation. *Theor. Appl. Climatol.* 105 (3–4), 311–323.
- Lindberg, F., Grimmond, C.S.B., Martilli, A., 2015. Sunlit fractions on urban facets – impact of spatial resolution and approach. *Urban Clim.* 12 (0), 65–84.
- Martilli, A., 2014. An idealized study of city structure, urban climate, energy consumption, and air quality. *Urban Clim.* 10, 430–446.
- Offerle, B., Grimmond, C., Fortuniak, K., Klysik, K., Oke, T., 2006. Temporal variations in heat fluxes over a central European city Centre. *Theor. Appl. Climatol.* 84, 103–115.
- Oke, T.R., 1982. The energetic basis of the urban heat island. *Q. J. R. Meteorol. Soc.* 108 (455), 1–24.
- Oke, T.R., Mills, G., Christen, A. and Voogt, J.A., 2017. Urban Climates.
- Park, J.K., Na, S.I., Park, J.H., 2012. Evaluation of surface heat flux based on satellite remote sensing and field measurement data. In 2012 Int. Geosci. Remote Sens. Symp. 1108–1111.
- Raupach, M.R., 1994. Simplified expressions for vegetation roughness length and zero-plane displacement as functions of canopy height and area index. *Bound.-Layer Meteorol.* 71 (1–2), 211–216.
- Sharmin, T., Steemers, K., Matzarakis, A., 2017. Microclimatic modelling in assessing the impact of urban geometry on urban thermal environment. *Sustain. Cities Soc.* 34, 293–308.

- Tian, Y., Zhou, W., Qian, Y., Zheng, Z., Yan, J., 2019. The effect of urban 2D and 3D morphology on air temperature in residential neighborhoods. *Landsc. Ecol.* 34 (5), 1161–1178.
- Vallati, A., Mauri, L., Colucci, C., Ocioñ, P., 2017. Effects of radiative exchange in an urban canyon on building surfaces' loads and temperatures. *Energ. Build.* 149, 260–271.
- Verma, S., 1989. Aerodynamic resistances to transfers of heat, mass and momentum. *Estimat. Areal Evapotranspirat.* 177, 13–20.
- Voogt, J.A., Grimmond, C., 2000. Modeling surface sensible heat flux using surface radiative temperatures in a simple urban area. *J. Appl. Meteorol.* 39 (10), 1679–1699.
- Wang, J., Zhou, W., Jiao, M., 2022. Location matters: planting urban trees in the right places improves cooling. *Front. Ecol. Environ.* 20 (3), 147–151.
- Ward, H.C., Evans, J.G., Grimmond, C.S.B., 2014. Multi-scale sensible heat fluxes in the suburban environment from large-aperture Scintillometry and Eddy covariance. *Bound.-Layer Meteorol.* 152 (1), 65–89.
- Weng, Q., Lu, D., Schubring, J., 2004. Estimation of land surface temperature–vegetation abundance relationship for urban heat island studies. *Remote Sens. Environ.* 89 (4), 467–483.
- Wong, M.S., et al., 2015. Modeling of anthropogenic heat flux using HJ-1B Chinese small satellite image: a study of heterogeneous urbanized areas in Hong Kong. *Geosci. Remote Sens. Lett. IEEE* 12 (7), 1466–1470.
- Xu, W., Wooster, M., Grimmond, C., 2008. Modelling of urban sensible heat flux at multiple spatial scales: a demonstration using airborne hyperspectral imagery of Shanghai and a temperature–emissivity separation approach. *Remote Sens. Environ.* 112 (9), 3493–3510.
- Yang, X., Li, Y., 2015. The impact of building density and building height heterogeneity on average urban albedo and street surface temperature. *Build. Environ.* 90 (0), 146–156.
- Yang, J., Wong, M.S., Menenti, M., Nichol, J., 2015a. Modeling the effective emissivity of the urban canopy using sky view factor. *ISPRS J. Photogramm. Remote Sens.* 105 (0), 211–219.
- Yang, J., Wong, M.S., Menenti, M., Nichol, J., 2015b. Study of the geometry effect on land surface temperature retrieval in urban environment. *ISPRS J. Photogramm. Remote Sens.* 109, 77–87.
- Yang, J., Wong, M.S., Menenti, M., 2016. Effects of urban geometry on turbulent fluxes: a remote sensing perspective. *IEEE Geosci. Remote Sens. Lett.* 13 (12), 1767–1771.
- Yang, J., et al., 2019. Parameterization of urban sensible heat flux from remotely sensed surface temperature: effects of surface structure. *Remote Sens.* 11 (11), 1347.
- Yang, J., et al., 2020. A semi-empirical method for estimating complete surface temperature from radiometric surface temperature, a study in Hong Kong city. *Remote Sens. Environ.* 237, 111540.
- Yang, J., et al., 2022. Characterizing the thermal effects of vegetation on urban surface temperature. *Urban Clim.* 44, 101204.
- Yu, K., et al., 2019. Study of the seasonal effect of building shadows on urban land surface temperatures based on remote sensing data. *Remote Sens.* 11 (5), 497.
- Yu, Z., et al., 2020. Quantifying seasonal and diurnal contributions of urban landscapes to heat energy dynamics. *Appl. Energy* 264, 114724.